



Technical Report No. 27

EFFECTS OF CLIMATE CHANGES ON WATER RESOURCES IN THE GLOMMA RIVER BASIN, NORWAY



Author names: Ingjerd Haddeland, Paul Christen Røhr, Hans Christian Udnæs

Date: 30.07.2011



WATCH is an Integrated Project Funded by the European Commission under the Sixth Framework Programme, Global Change and Ecosystems Thematic Priority Area (contract number: 036946). The WACH project started 01/02/2007 and will continue for 4 years.

Title:	
Authors:	Ingjerd Haddeland, Paul C. Røhr, Hans Christian Udnæs
Organisations:	Norwegian Water Resources and Energy Directorate (NVE), Glommen and Laagen Water Management Association (GLB)
Submission date:	30.07.2011
Function:	This report is an output from Work Package 6.4: Translating the global water cycle system to basins for water resources applications. More specifically, it covers work done in Task 6.4.4: The Glomma river.
Deliverable:	This report contributes to D 6.4.2 Final report test basins

Cover photos:

Left: Sula gauging station (Haddeland, 2007)

Right: Svanfoss dam (Haddeland, 2011)

Contents

- 1. Introduction 4
- 2. Study areas and input data 4
- 3. Models and setup 6
 - The hydrological model - HBV 6
 - The reservoir model – Mike11 7
- 4. Results and discussion 9
 - Snow and runoff..... 9
 - Hydropower production..... 12
 - Flood losses 14
- 5. Conclusions 15
- References..... 17

1. Introduction

In WATCH, a number of test basins across Europe have been used to study effects of climate change on a variety of water resource applications. Here, results from five small catchments within the Glomma River basin in Norway are presented; an area that provides hydropower services under threat of precipitation and temperature increases. The focus in this study is two-fold. First, the effects of climate change on snow and runoff is studied, including a comparison of hydrological simulation results using fine and large scale meteorological data. Second, effects of climate change on hydropower production in the northeastern part of the Glomma River basin are analyzed.

2. Study areas and input data

The Glomma River basin is the largest river basin in Norway, covering an area of 42,000 km²; see Figure 1. Mean annual precipitation is about 800 mm, and mean annual runoff at the outlet is estimated to be 530 mm. The annual runoff distribution is heavily influenced by snow accumulation and melt. Reservoir storage in the Glomma River basin is 3.5 km³, or about 16 percent of the mean annual flow. The hydropower plants in the basin produce about 2.5 TWh annually.

In this study, five catchments of varying size within the Glomma River basin are included; see also Figure 1 and Table 1. Hydropower production and flood loss analyses are performed for the Kursåsfossen hydropower plant, which is located near the Aursunden dam and reservoir in the one of the five catchments; namely the Aursunden catchment.

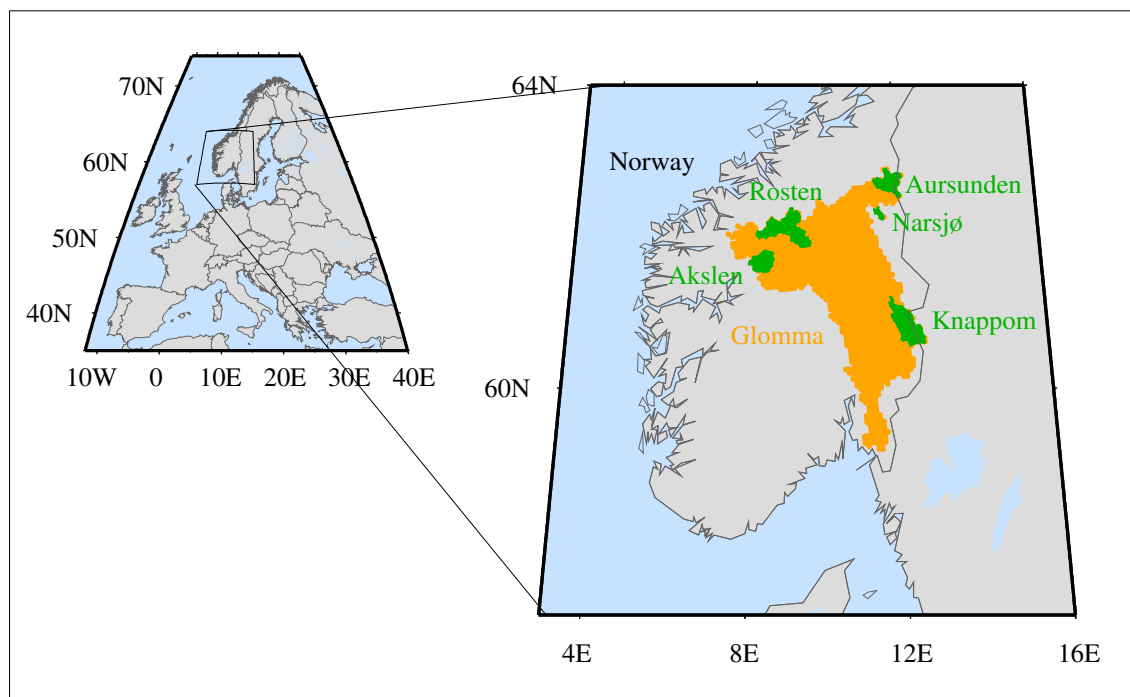


Figure 1: Location of the study catchments within the Glomma River basin. The hydropower plant Kursåsfossen is located at the outlet of the Aursunden catchment in the northeastern part of the Glomma River basin.

Precipitation and temperature at 1 km² spatial resolution and daily time steps for the period 1958-2000 were obtained from the Norwegian Meteorological Office (met.no). The gridded datasets are based on station observations, and includes undercatch corrections and orographic effects (Tveito et al., 2005). met.no has also made fine scale (1 km²) control and projection data for the Hadley (A2, B2) and ECHAM (B2) climate models available. These global climate model outputs were first dynamically downscaled using the HIRHAM regional climate model, and precipitation and temperature were thereafter bias corrected to the met.no fine scale observation based gridded historical dataset (Engen-Skaugen, 2007). In addition to the meteorological forcings at 1 km², the 0.5 degree WATCH Forcing Data (WFD, Weedon et al., 2011) (precipitation and temperature) were used. Also, climate projections made available through WATCH (i.e. ECHAM, CNRM, IPSL A2 and B1, 1961-2100), where precipitation and temperature are bias corrected to WFD (Hagemann et al., 2011) were used. The control period employed in this study is 1961-1990. Two projection periods are studied: 2021-2050 and 2071-2100. Among the emission scenarios used here, the A2 scenario globally results in the largest future temperature increases, and the B1 scenario results in the lowest temperature increases, see also Figure 2. Table 2 lists the meteorological input datasets used in this study.

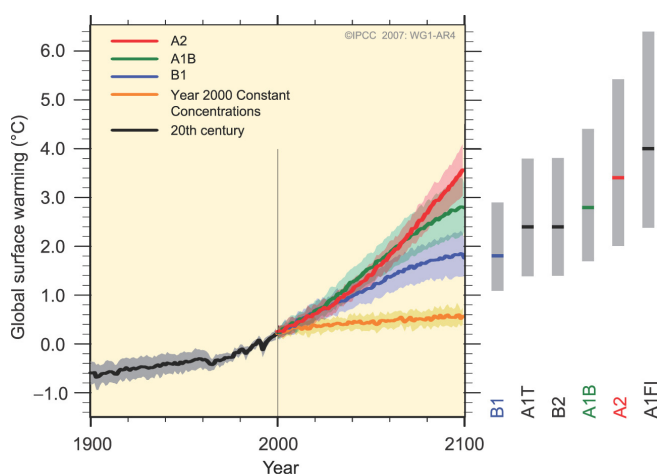


Figure 2: Solid lines are multi-model global averages of surface warming (relative to 1980–1999) for the scenarios shown as continuations of the 20th century simulations. Shading denotes the ± 1 standard deviation range of individual model annual averages. The orange line is for the experiment where concentrations were held constant at year 2000 values. The grey bars at right indicate the best estimate (solid line within each bar) and the likely range assessed for the six scenarios. The assessment of the best estimate and likely ranges in the grey bars includes the GCMs in the left part of the figure, as well as results from a hierarchy of independent models and observational constraints. Source: Figure SPM.5 in IPCC (2007).

Streamflow data for the study catchments are available since 1961 or earlier for all basins. Streamflow data, including naturalized data for Aursunden that is influenced by a reservoir, and information about operating rules at the Kursåsfossen hydropower plant are obtained from the Norwegian Water Resources and Energy Directorate (NVE) and Glommen and Laagen Water Management Association (GLB).

Table 1: Catchment information. Precipitation, temperature and runoff numbers are averaged over the period 1961-1990, and are based on fine and large scale meteorological data, and gauge measurements.

	Akslen	Rosten	Aursunden	Narsjø	Knappom
Area (km ²)	795	1828	843	119	1648
Elevation range (masl)	475 - 2462	319 - 2207	688 - 1564	737 - 1593	170 - 807
met.no temperature (°C)	-3.5	-1.8	-1.3	-2.7	1.1
Runoff (mm year ⁻¹)	946	557	750	589	425
met.no precipitation (mm year ⁻¹)	1179	869	991	921	794
WFD precipitation (mm year ⁻¹)	618	643	828	654	724

Table 2: Meteorological data and projections.

Source	met.no	met.no	met.no	WATCH	WATCH
Dataset / Climate model	met.no	Hadley	ECHAM	WFD	ECHAM, CNRM, IPSL
Scenario		A2, B2	B2		A2, B1
Scale	1 km ²	1 km ²	1 km ²	0.5 deg	0.5 deg
Time periods	1958 – 2011	1960 - 1990, 2071 - 2100	1960 – 1990, 2071 - 2100	1958 – 2001	1960 – 2100

3. Models and setup

The hydrological model - HBV

The hydrological model implemented for each of the five catchments is based on the HBV precipitation-runoff model, which has been extensively applied in the Nordic region since its development in the 1970s (Bergström, 1976). The original model has undergone numerous revisions and improvements, and today there are several implementations of HBV available. In the applications reported here, the “Nordic” HBV model (Killingveit and Sæthun, 1995; Sæthun, 1996) was used. This version represents a lumped catchment model in which the spatial structure of the catchment is not explicitly modelled. Ten equal area height zones from the hypsometric curve for the catchments are, however, used in the model snow routine, and land cover data is distributed by height zone. All processes contribute directly to runoff at the outlet without internal routing between elevation zones.

The catchment models were calibrated against observed streamflow (naturalized streamflow in the Aursunden catchment) for the period 1971-1980, using 1961-1970 as spin-up period. In the model calibrations presented here, PEST parameter estimation routines (Doherty, 2004) were used. The principal advantages of the PEST algorithm are that it is based on a relatively robust optimisation algorithm. In addition, the routines and documentation are freely available and have been widely applied

in the hydrological sciences (e.g. Liu et al, 2005; Lin and Radcliffe, 2005). A disadvantage of PEST is that it uses a local optimisation routine, such that the final values obtained may be dependent upon the initial parameter values used in the optimisation. To overcome this shortcoming, 15 randomly starting parameter sets were selected, and the optimal parameter set was chosen based on PEST calibration initiated by these starting datasets. Model performance was validated for the period 1981-1990, and the best parameter set was chosen based on Nash-Sutcliffe (NS) values and volume error in the validation period. For more details on the calibration procedure, see Lawrence et al. (2009). Calibration and validation were performed separately using local met.no data and WFD. The two resulting parameter sets were employed when using the input datasets (control and projection periods) made available by met.no and WATCH, respectively.

Table 3: Nash-Sutcliffe values, validation period (1981-1990).

	Akslen	Rosten	Aursunden	Narsjø	Knappom
met.no	0.86	0.91	0.85	0.87	0.77
WFD	0.86	0.88	0.88	0.81	0.78

In the calibration procedure input precipitation is corrected through a liquid and solid precipitation correction factor. The reasoning behind the correction is that catch errors and orographic effects on precipitation are not perfectly represented in the input datasets. Also, precipitation over an area will never be perfectly represented by the meteorological stations. In addition, the temperature gradient (wet and dry lapse rate) is adjusted somewhat. Figure 3 shows the original precipitation and temperature data and the corrected (calibrated) precipitation and temperature data for the control period (1961-1990). Averaged over the catchments, the met.no and WFD precipitation and temperature data show substantial differences, see Figure 3. In all catchments, met.no precipitation is higher than WFD precipitation, and met.no temperatures are lower than WFD temperatures. For precipitation, this is at least partly caused by met.no taking orographic effects into account when gridding the observations, whereas this is not included in WFD. In the Akslen catchment, which drains an area having large elevation differences, the mean annual WFD precipitation is much lower than the met.no precipitation, and is actually lower than the observed streamflow in the catchment (Table 1). A 0.5 deg WFD grid cell may cover larger areas than the fairly small catchments included in this study, which may additionally explain some of the precipitation and temperature differences between the two datasets. However, after calibration of the HBV catchment models, in which precipitation correction is arguably the most important factor, the average precipitation is much more similar (Figure 3).

The reservoir model – Mike11

A hydraulic model for the study area was established using the Mike11 modeling software from the Danish Hydraulic Institute (DHI). The modeling package can be used for simulation of one dimensional flow in rivers, irrigation systems, channels and other water bodies. Mike11 has been developed over the last 25 - 30 years and is now extensively used worldwide. Mike11 applied with the dynamic wave description solves the vertically integrated equations for conservation of continuity and momentum (the Saint Venant equations) (DHI, 2009) based on an implicit finite different scheme developed by Abbott and Ionescu (1967).

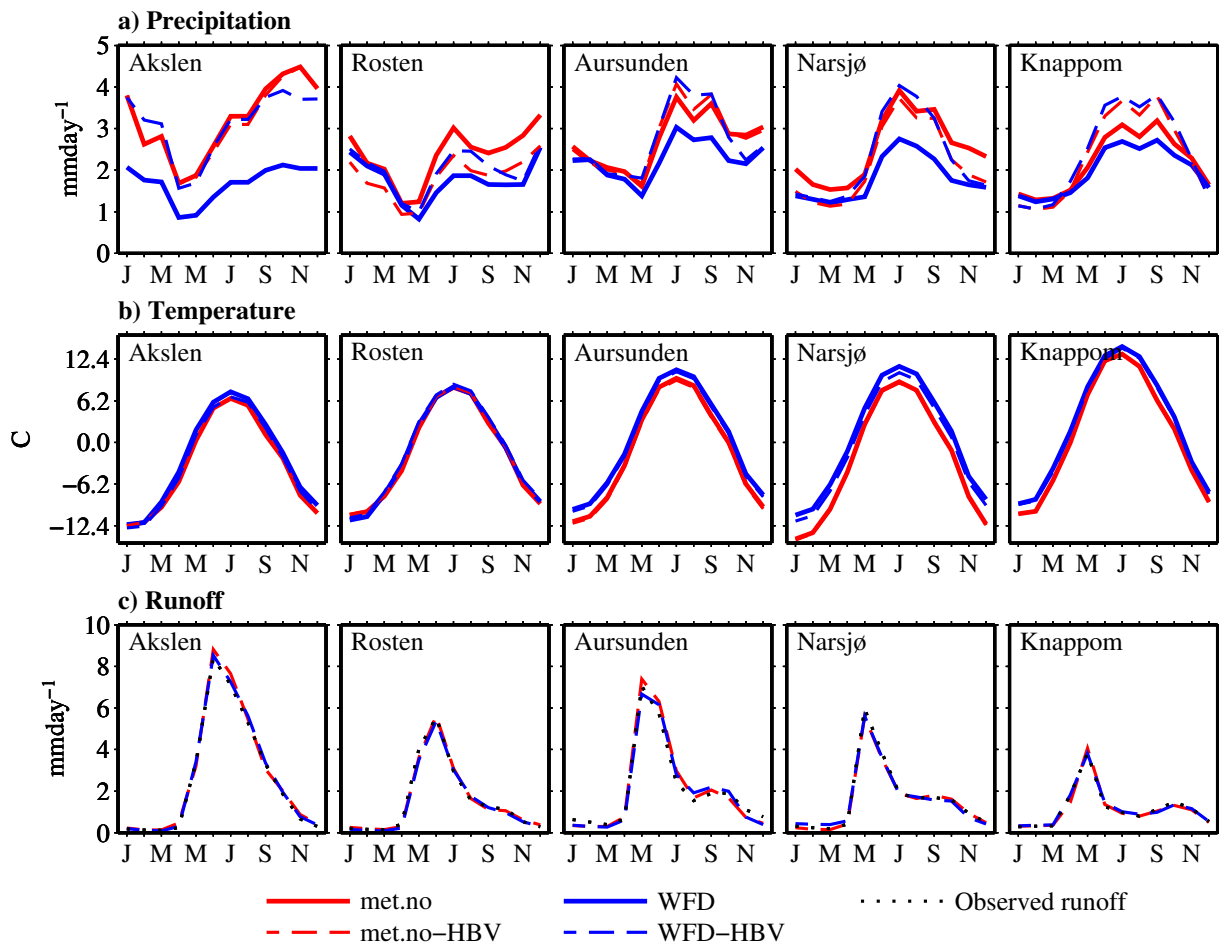


Figure 3: Mean monthly a) precipitation and b) temperature, 1961-1990, original data (met.no and WFD) and results after calibration (met.no-HBV and WFD-HBV). c) Mean monthly simulated and observed runoff, 1961-1990.

In this study, the Aursunden reservoir, the Kursåsfossen hydropower plant, and about 25 km of the downstream river are represented in the hydraulic model. The power plant is located about 800 m downstream of the reservoir. The operating rules of the Aursunden reservoir at the Kursåsfossen power plant, see Table 4, are included in the modeling scheme. The operating rules are simulated by use of the control structure module in Mike11 which gives restrictions on the operation of the reservoir.

Table 4: Operating rules at the Kursåsfossen hydropower plant.

No	Rule	Value
1	Maximum regulated water level	691.10 masl
2	Minimum regulated water level	685.20 masl
3	Capacity	28 m ³ s ⁻¹
4	Maximum discharge before freeze-up	13 m ³ s ⁻¹
5	Maximum daily increase in discharge after freeze-up	1 m ³ s ⁻¹
6	Environmental flow requirements	8 m ³ s ⁻¹

The Mike11 model for the Aursunden reservoir was verified against observed water levels at the reservoir as shown in Figure 4. For the verification simulations, inflow to the reservoir is taken from the HBV simulated runoff using the WATCH Forcing Data (WFD) as input. For calculation of freeze-up, which according to the operating rules influence reservoir releases during the freeze-up period, a simple river ice model is implemented. The model uses air temperature as input and takes both freezing and melting in the freeze-up period into account.

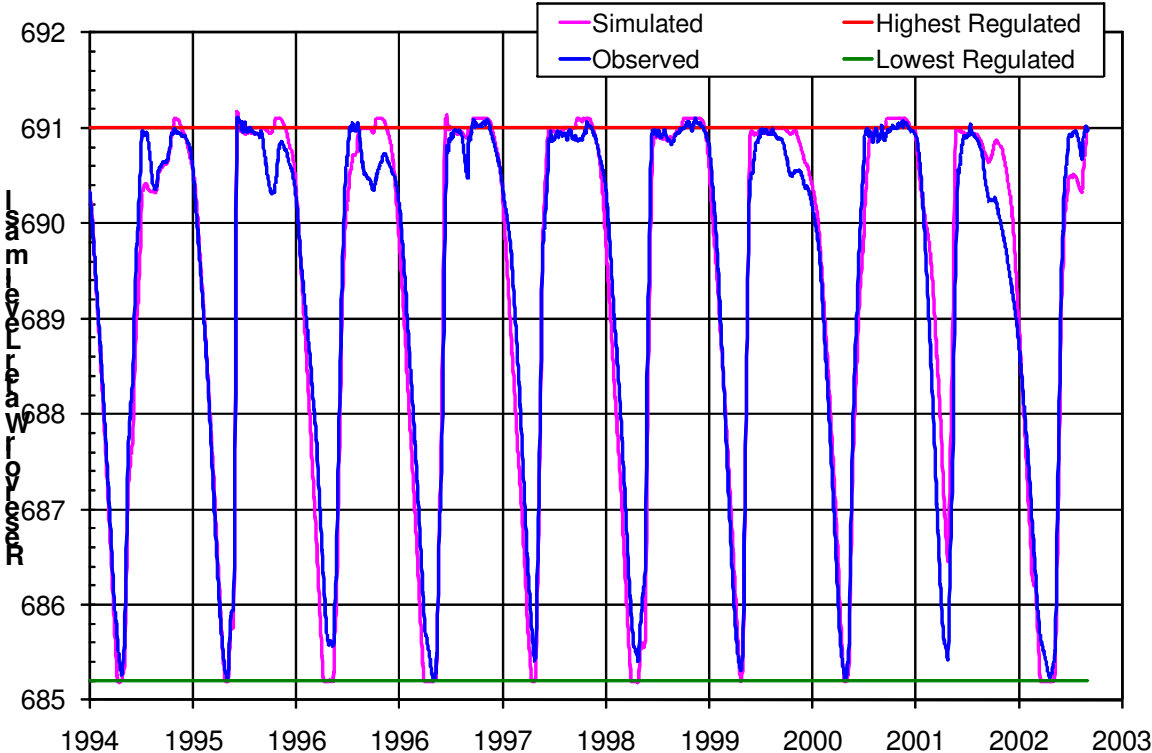


Figure 4: Observed and simulated water level at the Lake Aursunden Reservoir.

After adaption and verification of the reservoir model for the Aursunden catchment, the model was run for a selection of simulated inflow the reservoir for the period 1960-2100. The HBV simulated runoff for Aursunden was used as input to the Mike11 reservoir model. That is, inflow to the catchment equals HBV simulated runoff using meteorological data (precipitation and temperature) from three climate models; ECHAM, IPSL and CNRM3, and two emission scenarios; A2 and B1 (see above). The result from the Mike11 model is simulated runoff from the reservoir which constitutes two components: 1) discharge through the hydropower plant and 2) flood loss. Power production and flood loss are calculated for each day in the simulation period.

4. Results and discussion

Snow and runoff

Comparing the control and projection period results for precipitation and runoff (Figure 5), it is apparent that both precipitation and runoff increase in the study catchments for the majority of the climate projections. Figure 5 compares the overlapping time periods of the input datasets, i.e. 1961-1990 and 2071-2100. All WATCH climate projections, and corresponding hydrological simulations, indicate increases in precipitation, and substantial increases in runoff. The A2 scenarios, not surprisingly, show larger percentage changes than the B1 scenarios, but differences exist among the climate models for

the same emission scenario. The Hadley model predicts the smallest precipitation increases, and according to both Hadley A2 and B2 the Rosten catchment annual precipitation is predicted to decrease in the future. Consequently, runoff projections based on fine scale Hadley A2 and B2 show the smallest runoff increases, and for some catchments (Aursunden and Rosten) Hadley A2 results in decreased runoff. The fine scale ECHAM B2 precipitation scenarios are closer to the large scale WATCH precipitation scenarios. However, a direct comparison is not possible since the climate models and emission scenarios used are not overlapping (the same combination of climate model and emission scenario at fine and large scales were not available at the time of this study). Hence, it cannot be concluded whether the resulting differences in runoff are mainly caused by differences in spatial scale and hence spatial coverage of the input datasets for each catchment, or by differences in the climate models and emission scenarios.

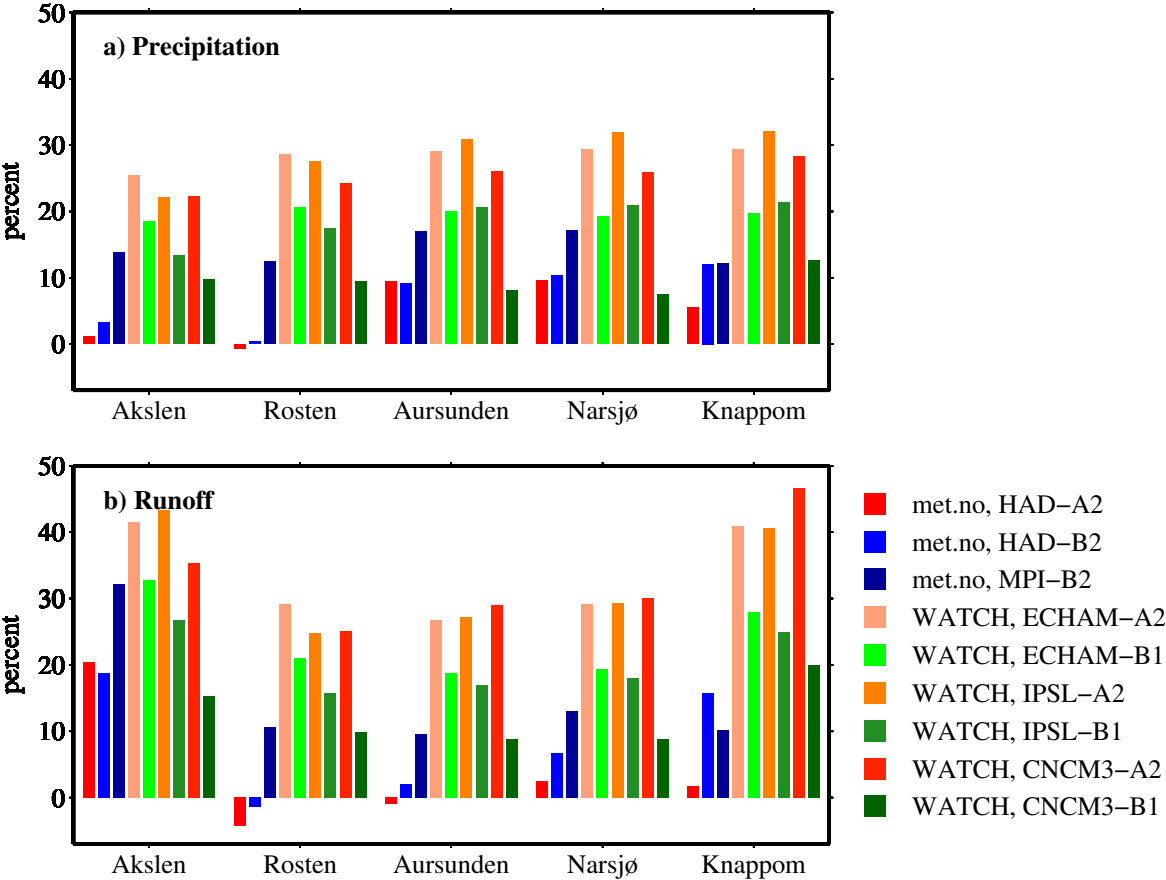


Figure 5: Mean annual changes in a) precipitation (bias corrected climate model output) and b) runoff (HBV model output) for three fine scale (met.no) and 6 large scale (WATCH) datasets. 2071-2100 compared to 1961-1990.

Mean monthly precipitation, temperature, snow water equivalent (SWE) and runoff presented in Figure 6 are results after HBV calibration, and the same calibration parameters (e.g. precipitation correction factors) are used for the control and projection periods. All climate models predict future temperature increases in all catchments (Figure 6b). The combination of temperature and precipitation changes result in somewhat different effects when looking at snow accumulation and melt in the catchments (Figure 6c). In the low elevation Knappom catchment (median elevation is 410 masl), snow water equivalent (SWE) throughout the winter season is predicted to decrease, and winter runoff increases. In the Akslen catchment (median elevation is 1466 masl), which drains the highest mountains in Norway, the results demonstrate the sensitivity of water balance components to the combination of temperature

and precipitation throughout the year. Winter temperatures are in general low in the Akslen catchment, and hence a slight increase in temperature affects snowfall and snowmelt less than in e.g. the Knappom catchment. Given the low winter temperatures, which stay well below freezing also in future projections, increased winter precipitation (WATCH projections) lead to higher maximum SWE values. However, according to the fine scale climate projections winter precipitation is hardly changing in the future, and hence higher temperatures result in lower maximum SWE. This is again reflected in the runoff numbers; the higher snow amounts, the more runoff during the snowmelt season (typically May and June).

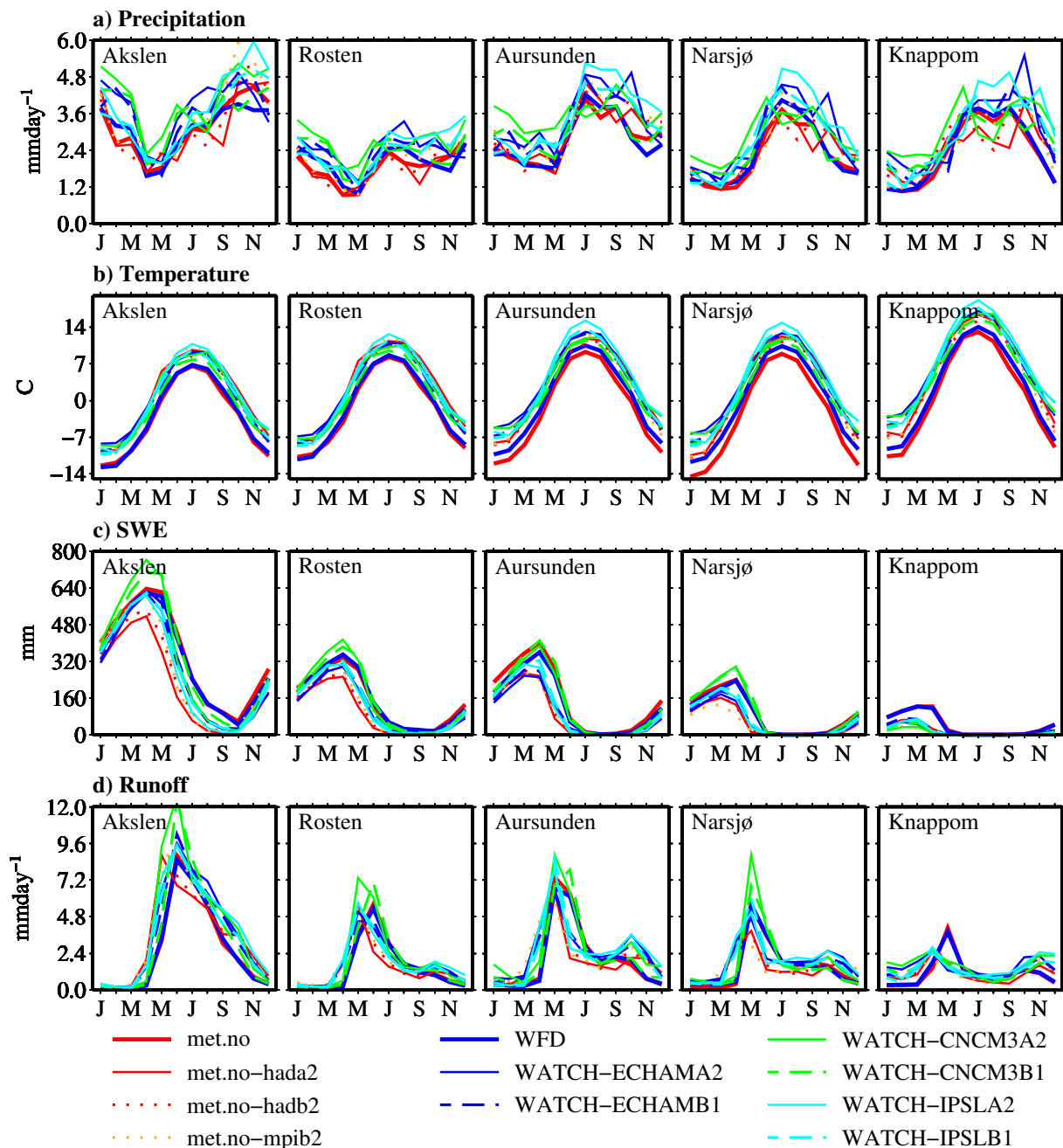


Figure 6: Mean monthly a) precipitation, b) temperature, c) snow water equivalent and d) runoff, 1961-1990, and 2071-2100, met.no and WFD. All results after HBV calibration.

The results indicate the highest SWE increases in most catchments are predicted when using CNCM3 A2 and B1 input. CNCM3 predicts the highest precipitation increases (Figure 6a) during the winter

months (especially January, February, March), which is reflected in SWE (Figure 6c). However, the SWE projections are also a result of CNCM3 in general predicting lower temperature increases than the other climate models (Figure 6b). Hence lower increases in runoff during the winter months but higher runoff numbers during the snowmelt months. This especially affects the CNCM3 B1 results, which is at the lower end in all catchments.

In most catchments and for most projections, runoff in the summer after the main snowmelt season is predicted to decrease in the future. Apart from the effect this may have on future droughts (see Wong et al., 2011) it will also affect the hydropower sector. Timing and amount are crucial for hydropower production, and is further explored in the next section, using runoff results for the Aursunden catchment. These results are presented in Figure 7 so that the different projections are possible to distinguish.

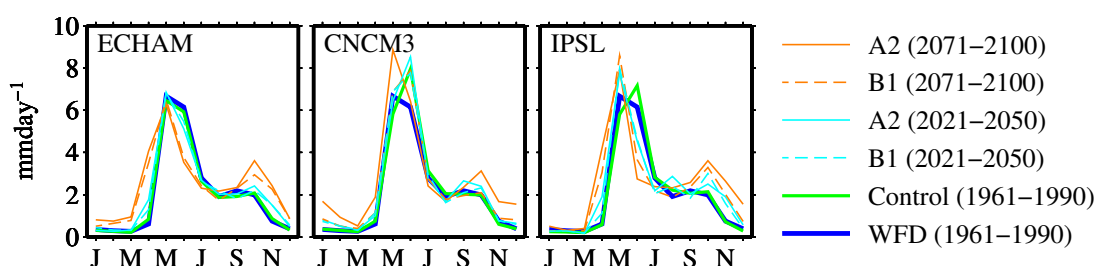


Figure 7: Runoff results for the Aursunden catchment using precipitation and temperature from three climate models and two emission scenarios. Runoff results using WFD (control period) are included in all panels for reference purposes.

Hydropower production

Annual hydropower production statistics for the control and projection periods are presented in Figures 8 and 9, which gives a graphical and a tabular presentation of some main figures for the Kuråsossen power plant at the outlet of the Aursunden reservoir. Figure 8 includes information on simulated median annual power production at Kuråsossen, whereas Figure 9 presents the simulated mean annual power production numbers. All six simulated runoff projections (Figure 7) results in increased power production, compared to the control period. For the A2 emission scenario, power production increases between 10 and 14 percent, with the highest increase predicted when using precipitation and temperature input from the ECHAM model. The B1 emission scenario gives an increase in power production between 5 and 12 percent. The CNCM3 climate model indicates that the major part of the increase will take part between now and 2021-250, with only marginal increases in the following period.

The increases in power production are closely related to future increases in precipitation and runoff (Figures 5 and 7). In the Aursunden catchment, precipitation and runoff are both projected to increase between 10 and 30 percent towards the end of the century for the climate models and emission scenarios taken into account in the hydropower simulations. As mentioned above, the predicted increases in hydropower production (2071 -2100 compared to 1961-1990) are between 5 and 14 percent. Some reasons that the projected relative increases in power production are lower than the projected relative increases in inflow to the reservoir are discussed below.

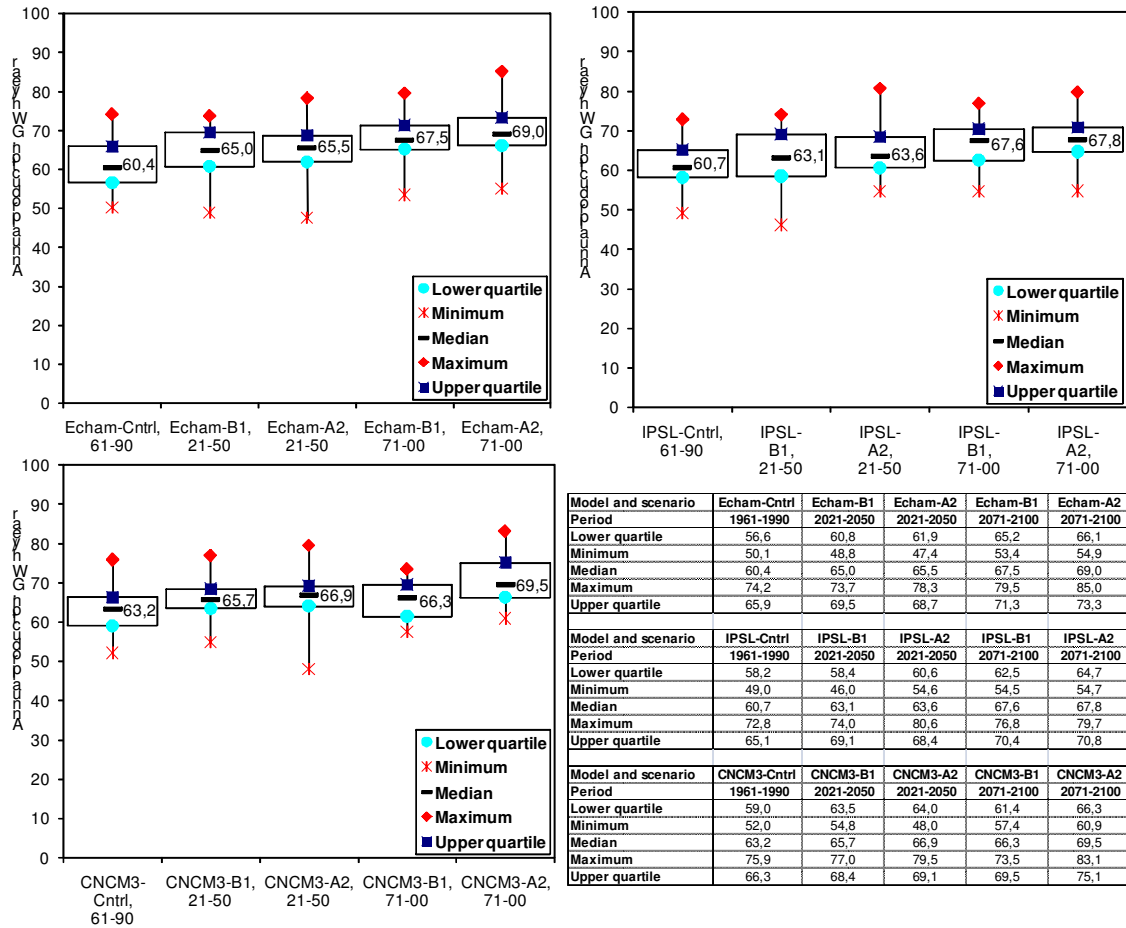


Figure 8: Graphical and tabular presentation of production statistics for Kuråsossen Power Plant using inflow based on precipitation and temperature from three climate models and two emission scenarios.

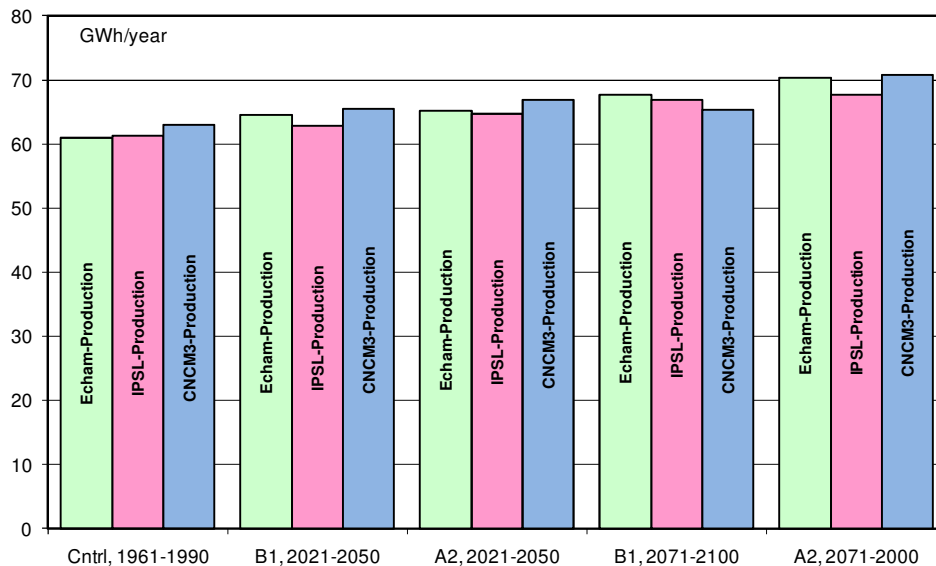


Figure 9: Mean annual simulated power production for the B1 and A2 emission scenario for the control period and the 2021-2050 and 2071-2100 projection periods.

Flood losses

The Aursunden dam and the Kuråsfossen power plant were constructed in order to optimize the use of available water resources, and at the same time take environmental issues (e.g. environmental flows) into account. It is not possible to utilize all available water for power production, and some flood loss is accepted. Annual flood losses for the control and the projection periods are presented in Figure 9. It gives a graphical and a tabular presentation of the major figures of the flood loss for the Kuråsfossen power plant at the Aursunden reservoir. All climate models and emission scenarios indicate an increase in flood loss. For the B1 emission scenario, the increase in flood loss varies from about 40 to 90 percent for the climate projections. The A2 emission scenario indicates an increase in flood loss between 130 and 175 percent. Generally, most of the increase in flood loss occurs after the 2021-2050 period. The increase in flood loss is also illustrated in Figure 11. A wetter future climate results in increased inflow to the reservoir, and hence the flood loss will also increase.

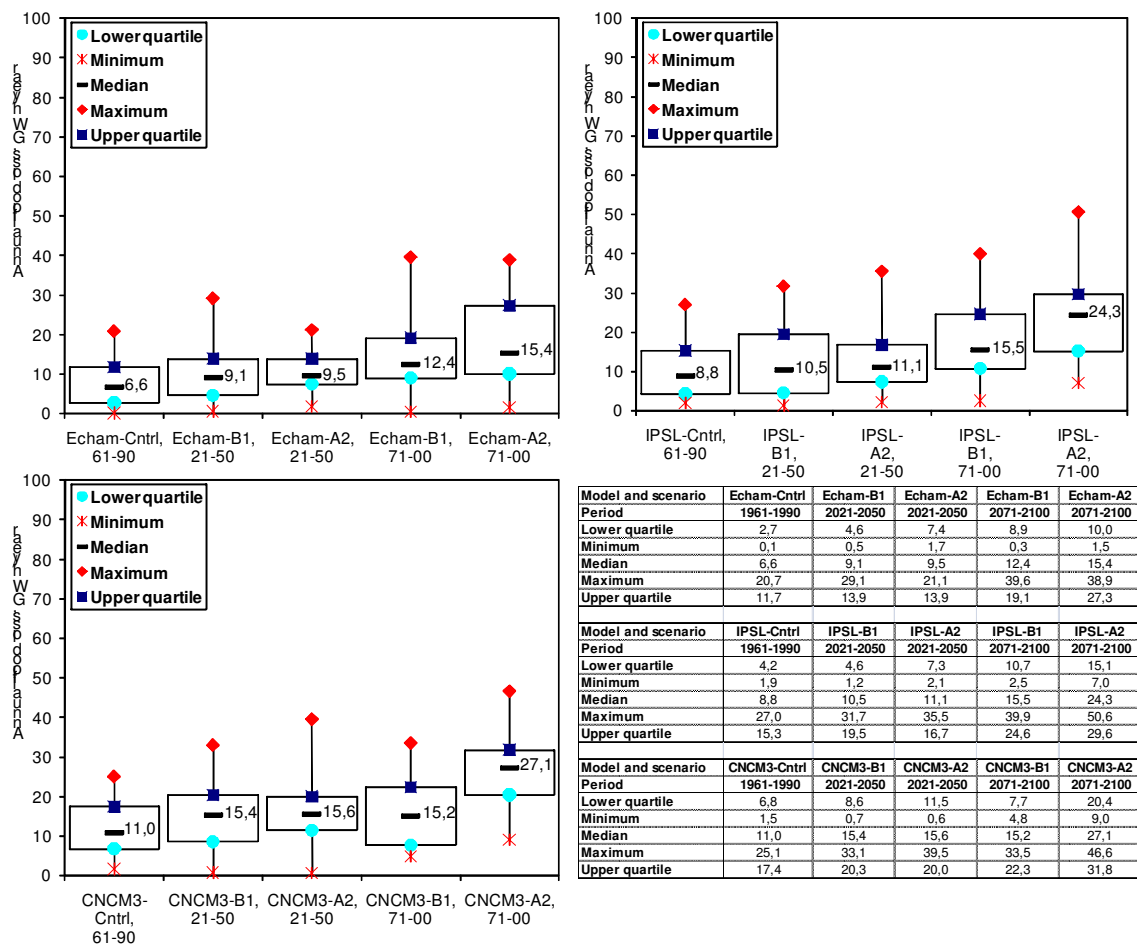


Figure 10: Graphical and tabular presentation of flood loss statistics for Kuråsfossen hydropower plant using inflow based on precipitation and temperature from three climate models and two emission scenarios.

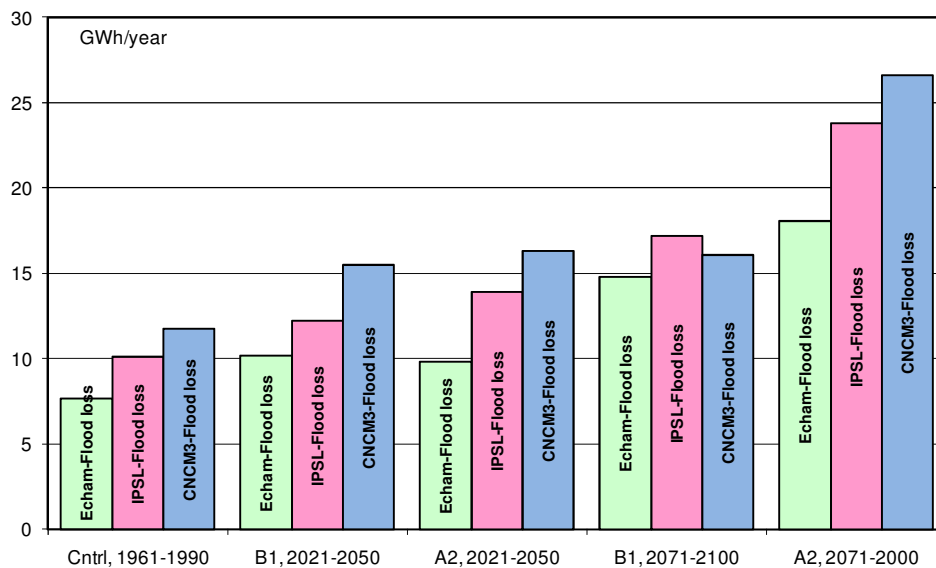


Figure 11: Mean annual simulated flood loss for the B1 and A2 emission scenario for the control period and the 2021-2050 and 2071-2100 projection periods.

The future increases in flood loss might be reduced, and hence future power production might be increased, if current operating rules are adapted to future climate changes. Also, modifications of current installations might reduce flood losses and increase power production. Adaptation strategies have not been studied in detail here, but it is likely that more intense power production in the autumn period would lead to smaller flood losses in the spring. Also, the restrictions in the freeze-up period could be reduced to some degree; allowing a somewhat later freeze-up. Test of various climate change adaption strategies should be a topic for further studies.

5. Conclusions

Using the fine scale met.no and the large scale WFD precipitation and temperature data as input to HBV hydrological models for five catchments within the Glomma River basin both result in good runoff simulations. However, the good results are only achieved after model calibration in which solid and liquid precipitation is corrected. In all five catchments studied here, the WFD precipitation is apparently too low, which is especially apparent in the Akslen catchment where mean annual precipitation according to WFD is lower than observed mean annual runoff. The met.no precipitation is also corrected, and in two of the basins the precipitation values are lowered during the calibration process. The precipitation distributions throughout the year is apparently good for both precipitation datasets, and after calibration Nash-Sutcliffe (NS) values for the HBV simulated runoff (compared to observations) are between 0.77 and 0.91.

Future projected changes in temperature and precipitation result in somewhat different effects when looking at snow water equivalent (SWE) and runoff in the catchments. In the Knappom catchment, where the median elevation is 410 masl, SWE decreases throughout the winter season, winter runoff increases, and spring runoff decreases. In the higher elevation Akslen catchment (median elevation is 1466 masl), increased winter precipitation lead to higher maximum SWE values, and hence increased spring runoff.

The reservoir model Mike-11 give a good fit between the simulated and the observed water level at the Lake Aursunden Reservoir. Simulation of hydropower production at Aursunden indicates increased production for all emission scenarios and all climate models. It should be noted, though, that the extent of the increase may be somewhat difficult to estimate in details since the reservoir operation is somewhat influenced by subjective decisions from the operators difficult to implement in a mathematical simulation.

References

- Abbott, M.B. and F. Ionescu, 1967, On the numerical computation of nearly-horizontal flows. *J. Hyd. Res.*, 5, 97-117.
- Bergström, S. 1976, Development and application of a conceptual runoff model for Scandinavian catchments. SMHI Report RH07.
- DHI, 2009, Mike11 – A modelling system for Rivers and Channels. Reference Manual. Danish Hydraulic Institute, Denmark.
- Doherty, J., 2004, PEST: Model Independent Parameter Estimation. Fifth edition of user manual. Watermark Numerical Computing, Brisbane, Australia.
- Engen-Skaugen, T., 2007, Refinement of dynamically downscaled precipitation and temperature scenarios. *Climatic Change*, 84, 365-382. DOI:10.1007/s10584-007-9251-6.
- Hagemann, S., C. Chen, J.O. Haerter, J. Heinke, D. Gerten, and C. Piani, 2011, Impact of a statistical bias correction on the projected hydrological changes obtained from three GCMs and two hydrology models, *J. Hydrometeor.*, 10.1175/2011JHM1336.1, in press.
- IPCC, 2007, Summary for Policymakers. In: *Climate Change 2007: The Physical Science Basis. Contribution of Working Group I to the Fourth Assessment Report of the Intergovernmental Panel on Climate Change* [Solomon, S., D. Qin, M. Manning, Z. Chen, M. Marquis, K.B. Averyt, M. Tignor and H.L. Miller (eds.)]. Cambridge University Press, Cambridge, United Kingdom and New York, NY, USA.
- Killingveit, Å. and N. R. Sælthun. 1995, Hydrological models. In *Hydropower Development 7: Hydrology*. Trondheim: Norwegian Institute of Technology, pp. 99-128.
- Lawrence, D., I. Haddeland, and E. Langsholt, 2009, Calibration of HBV hydrological models using PEST parameter estimation, *NVE Report 1-2009*, Norwegian Water Recourses and Energy Directorate, Oslo, Norway, 44 pp.
- Lawrence, D., and I. Haddeland, 2011, Uncertainty in catchment-scale HBV modelling of climate change impacts on peak flows in Norway, *Hydrology Research*, 42, doi: 10.2166/nh.2011.010.
- Lin, Z., and D.E. Radcliffe, 2005, Automatic calibration and predictive uncertainty analysis of a semidistributed watershed model. *Vadose Zone J.*, 5, 248-260, doi:10.2136/vzj2004.0025.
- Liu, Y.B., S. Gebremeskel, S., De Smedt., F., Hoffmann, L., and L. Pfister, 2006, Predicting storm runoff from different land-use classes using a geographical information system-based distributed model. *Hydrol. Process.* 20, 533-548, doi: 10.1002/hyp.5920.
- Sælthun, N.S., 1996, The Nordic HBV Model. *NVE Publication no. 07-1996*, Norwegian Water Recourses and Energy Directorate, Oslo, Norway, 26 pp.
- Tveito, O.E., Bjordal, I., Skjelvag, A.O., and B. Aune, 2005, A GIS-based agro-ecological decision system based on gridded climatology. *Meteorological Applications*, 12, 57-68.
- Weedon, G.P., S. Gomes, P. Viterbo, J. Shuttleworth, E. Blyth, H. Österle, J.C. Adam, N. Bellouin, O. Boucher, and M. Best, 2011, Creation of the WATCH Forcing Data and its use to assess global and regional reference crop evaporation over land during the twentieth century, *J. Hydrometeor.* doi: 10.1175/2011JHM1369.1 (in press).
- Wong, W.K., S. Beldring, T. Engen-Skaugen, I. Haddeland, and H. Hisdal, 2011, Climate change effects on spatiotemporal patterns of hydroclimatological summer droughts in Norway, *J. Hydrometeor.*, doi: 10.1175/2011JHM1357.1 (in press)